EUROPEAN ORGANIZATION FOR NUCLEAR RESEARCH

CERN–PH–EP/2008–003
8th February 2008

# Direct Measurement of the Gluon Polarisation in the Nucleon via Charmed Meson Production

*The COMPASS Collaboration*

**Abstract**

We present the first measurement of the gluon polarisation in the nucleon based on the photon–gluon fusion process tagged by charmed meson production and decay to charged $K$ and $\pi$. The data were collected in polarised muon scattering off a polarised deuteron target by the COMPASS collaboration at CERN during 2002–2004. The result of this LO analysis is $\left\langle \frac{\Delta g}{g} \right\rangle_x = -0.47 \pm 0.44(\text{stat}) \pm 0.15(\text{syst})$ at $\langle x \rangle \approx 0.11$ and a scale $\mu^2 \approx 13\,(\text{GeV}/c)^2$.

PACS 13.60.-r, 13.88.+e, 14.20.Dh, 14.70.Dj

*submitted to Physical Review Letters*

# The COMPASS Collaboration

M. Alekseev[32)], V.Yu. Alexakhin[8)], Yu. Alexandrov[18)], G.D. Alexeev[8)], A. Amoroso[30)], A. Arbuzov[8)], B. Badełek[33)], F. Balestra[30)], J. Ball[25)], J. Barth[4)], G. Baum[1)], Y. Bedfer[25)], C. Bernet[25)], R. Bertini[30)], M. Bettinelli[19)], R. Birsa[27)], J. Bisplinghoff[3)], P. Bordalo[15,a)], F. Bradamante[28)], A. Bravar[16,27)], A. Bressan[28,11)], G. Brona[33)], E. Burtin[25)], M.P. Bussa[30)], A. Chapiro[29)], M. Chiosso[30)], A. Cicuttin[29)], M. Colantoni[31)], S. Costa[30,+)], M.L. Crespo[29)], S. Dalla Torre[27)], T. Dafni[25)], S. Das[7)], S.S. Dasgupta[6)], R. De Masi[20)], N. Dedek[19)], O.Yu. Denisov[31,b)], L. Dhara[7)], V. Diaz[29)], A.M. Dinkelbach[20)], S.V. Donskov[24)], V.A. Dorofeev[24)], N. Doshita[21)], V. Duic[28)], W. Dünnweber[19)], P.D. Eversheim[3)], W. Eyrich[9)], M. Faessler[19)], V. Falaleev[11)], A. Ferrero[30,11)], L. Ferrero[30)], M. Finger[22)], M. Finger jr.[8)], H. Fischer[10)], C. Franco[15)], J. Franz[10)], J.M. Friedrich[20)], V. Frolov[30,b)], R. Garfagnini[30)], F. Gautheron[1)], O.P. Gavrichtchouk[8)], R. Gazda[33)], S. Gerassimov[18,20)], R. Geyer[19)], M. Giorgi[28)], B. Gobbo[27)], S. Goertz[2,4)], A.M. Gorin[24)], S. Grabmüller[20)], O.A. Grajek[33)], A. Grasso[30)], B. Grube[20)], R. Gushterski[8)], A. Guskov[8)], F. Haas[20)], J. Hannappel[4)], D. von Harrach[16)], T. Hasegawa[17)], J. Heckmann[2)], S. Hedicke[10)], F.H. Heinsius[10)], R. Hermann[16)], C. Heß[2)], F. Hinterberger[3)], M. von Hodenberg[10)], N. Horikawa[21,c)], S. Horikawa[21)], N. d'Hose[25)], C. Ilgner[19)], A.I. Ioukaev[8)], S. Ishimoto[21)], O. Ivanov[8)], Yu. Ivanshin[8)], T. Iwata[21,35)], R. Jahn[3)], A. Janata[8)], P. Jasinski[16)], R. Joosten[3)], N.I. Jouravlev[8)], E. Kabuß[16)], D. Kang[10)], B. Ketzer[20)], G.V. Khaustov[24)], Yu.A. Khokhlov[24)], Yu. Kisselev[1,2)], F. Klein[4)], K. Klimaszewski[33)], S. Koblitz[16)], J.H. Koivuniemi[13,2)], V.N. Kolosov[24)], E.V. Komissarov[8)], K. Kondo[21)], K. Königsmann[10)], I. Konorov[18,20)], V.F. Konstantinov[24)], A.S. Korentchenko[8)], A. Korzenev[16,b)], A.M. Kotzinian[8,30)], N.A. Koutchinski[8)], O. Kouznetsov[8,25)], A. Kral[23)], N.P. Kravchuk[8)], Z.V. Kroumchtein[8)], R. Kuhn[20)], F. Kunne[25)], K. Kurek[33)], M.E. Ladygin[24)], M. Lamanna[11,28)], J.M. Le Goff[25)], A.A. Lednev[24)], A. Lehmann[9)], S. Levorato[28)], J. Lichtenstadt[26)], T. Liska[23)], I. Ludwig[10)], A. Maggiora[31)], M. Maggiora[30)], A. Magnon[25)], G.K. Mallot[11)], A. Mann[20)], C. Marchand[25)], J. Marroncle[25)], A. Martin[28)], J. Marzec[34)], F. Massmann[3)], T. Matsuda[17)], A.N. Maximov[8,+)], W. Meyer[2)], A. Mielech[27,33)], Yu.V. Mikhailov[24)], M.A. Moinester[26)], A. Mutter[10,16)], A. Nagaytsev[8)], T. Nagel[20)], O. Nähle[3)], J. Nassalski[33)], S. Neliba[23)], F. Nerling[10)], S. Neubert[20)], D.P. Neyret[25)], V.I. Nikolaenko[24)], K. Nikolaev[8)], A.G. Olshevsky[8)], M. Ostrick[4)], A. Padee[34)], P. Pagano[28)], S. Panebianco[25)], R. Panknin[4)], D. Panzieri[32)], S. Paul[20)], B. Pawlukiewicz-Kaminska[33)], D.V. Peshekhonov[8)], V.D. Peshekhonov[8)], G. Piragino[30)], S. Platchkov[25)], J. Pochodzalla[16)], J. Polak[14)], V.A. Polyakov[24)], J. Pretz[4)], S. Procureur[25)], C. Quintans[15)], J.-F. Rajotte[19)], S. Ramos[15,a)], V. Rapatsky[8)], G. Reicherz[2)], D. Reggiani[11)], A. Richter[9)], F. Robinet[25)], E. Rocco[27,30)], E. Rondio[33)], A.M. Rozhdestvensky[8)], D.I. Ryabchikov[24)], V.D. Samoylenko[24)], A. Sandacz[33)], H. Santos[15,a)], M.G. Sapozhnikov[8)], S. Sarkar[7)], I.A. Savin[8)], P. Schiavon[28)], C. Schill[10)], L. Schmitt[20,d)], P. Schönmeier[9)], W. Schröder[9)], O.Yu. Shevchenko[8)], H.-W. Siebert[12,16)], L. Silva[15)], L. Sinha[7)], A.N. Sissakian[8)], M. Slunecka[8)], G.I. Smirnov[8)], S. Sosio[30)], F. Sozzi[28)], A. Srnka[5)], F. Stinzing[9)], M. Stolarski[33,10)], V.P. Sugonyaev[24)], M. Sulc[14)], R. Sulej[34)], V.V. Tchalishev[8)], S. Tessaro[27)], F. Tessarotto[27)], A. Teufel[9)], L.G. Tkatchev[8)], G. Venugopal[3)], M. Virius[23)], N.V. Vlassov[8)], A. Vossen[10)], R. Webb[9)], E. Weise[3,10)], Q. Weitzel[20)], R. Windmolders[4)], S. Wirth[9)], W. Wiślicki[33)], H. Wollny[10)], K. Zaremba[34)], M. Zavertyaev[18)], E. Zemlyanichkina[8)], J. Zhao[16,27)], R. Ziegler[3)] and A. Zvyagin[19)]

[1] Universität Bielefeld, Fakultät für Physik, 33501 Bielefeld, Germany[e]
[2] Universität Bochum, Institut für Experimentalphysik, 44780 Bochum, Germany[e]
[3] Universität Bonn, Helmholtz-Institut für Strahlen- und Kernphysik, 53115 Bonn, Germany[e]
[4] Universität Bonn, Physikalisches Institut, 53115 Bonn, Germany[e]
[5] Institute of Scientific Instruments, AS CR, 61264 Brno, Czech Republic[f]
[6] Burdwan University, Burdwan 713104, India[g]
[7] Matrivani Institute of Experimental Research & Education, Calcutta-700 030, India[h]
[8] Joint Institute for Nuclear Research, 141980 Dubna, Moscow region, Russia
[9] Universität Erlangen–Nürnberg, Physikalisches Institut, 91054 Erlangen, Germany[e]
[10] Universität Freiburg, Physikalisches Institut, 79104 Freiburg, Germany[e]
[11] CERN, 1211 Geneva 23, Switzerland
[12] Universität Heidelberg, Physikalisches Institut, 69120 Heidelberg, Germany[e]
[13] Helsinki University of Technology, Low Temperature Laboratory, 02015 HUT, Finland and University of Helsinki, Helsinki Institute of Physics, 00014 Helsinki, Finland
[14] Technical University in Liberec, 46117 Liberec, Czech Republic[f]
[15] LIP, 1000-149 Lisbon, Portugal[i]
[16] Universität Mainz, Institut für Kernphysik, 55099 Mainz, Germany[e]
[17] University of Miyazaki, Miyazaki 889-2192, Japan[j]
[18] Lebedev Physical Institute, 119991 Moscow, Russia
[19] Ludwig-Maximilians-Universität München, Department für Physik, 80799 Munich, Germany[e,k]
[20] Technische Universität München, Physik Department, 85748 Garching, Germany[e,k]
[21] Nagoya University, 464 Nagoya, Japan[j]
[22] Charles University, Faculty of Mathematics and Physics, 18000 Prague, Czech Republic[f]
[23] Czech Technical University in Prague, 16636 Prague, Czech Republic[f]
[24] State Research Center of the Russian Federation, Institute for High Energy Physics, 142281 Protvino, Russia
[25] CEA DAPNIA/SPhN Saclay, 91191 Gif-sur-Yvette, France
[26] Tel Aviv University, School of Physics and Astronomy, 69978 Tel Aviv, Israel[l]
[27] Trieste Section of INFN, 34127 Trieste, Italy
[28] University of Trieste, Department of Physics and Trieste Section of INFN, 34127 Trieste, Italy
[29] Abdus Salam ICTP and Trieste Section of INFN, 34127 Trieste, Italy
[30] University of Turin, Department of Physics and Torino Section of INFN, 10125 Turin, Italy
[31] Torino Section of INFN, 10125 Turin, Italy
[32] University of Eastern Piedmont, 1500 Alessandria, and Torino Section of INFN, 10125 Turin, Italy
[33] Sołtan Institute for Nuclear Studies and Warsaw University, 00-681 Warsaw, Poland[m]
[34] Warsaw University of Technology, Institute of Radioelectronics, 00-665 Warsaw, Poland[n]
[35] Yamagata University, Yamagata, 992-8510 Japan[j]
[+] Deceased
[a] Also at IST, Universidade Técnica de Lisboa, Lisbon, Portugal
[b] On leave of absence from JINR Dubna
[c] Also at Chubu University, Kasugai, Aichi, 487-8501 Japan
[d] Also at GSI mbH, Planckstr. 1, D-64291 Darmstadt, Germany
[e] Supported by the German Bundesministerium für Bildung und Forschung
[f] Suppported by Czech Republic MEYS grants ME492 and LA242
[g] Supported by DST-FIST II grants, Govt. of India
[h] Supported by the Shailabala Biswas Education Trust
[i] Supported by the Portuguese FCT - Fundação para a Ciência e Tecnologia grants POCTI/FNU/49501/2002 and POCTI/FNU/50192/2003
[j] Supported by the Ministry of Education, Culture, Sports, Science and Technology, Japan, Grant-in-Aid for Specially Promoted Research No. 18002006; Daikou Foundation and Yamada Foundation
[k] Supported by the DFG cluster of excellence 'Origin and Structure of the Universe' (www.universe-cluster.de)
[l] Supported by the Israel Science Foundation, founded by the Israel Academy of Sciences and Humanities
[m] Supported by Ministry of Science and Higher Education grant 41/N-CERN/2007/0 and the MNII

Pioneering experiments on the spin structure of the nucleon performed in the seventies [1] were followed by the EMC experiment at CERN which obtained a stunning conclusion on the quark contribution to the proton spin [2]. This result triggered extensive studies of the spin structure of the nucleon in lepton scattering experiments at CERN by the SMC [3] and COMPASS [4] SLAC [5], DESY (HERMES) [6] and JLAB [7] as well as in polarised proton-proton collisions at RHIC [8, 9]. The results of these studies confirmed the validity of the Bjorken sum rule and the violation of the Ellis–Jaffe sum rule. In addition, the parton helicity distributions in the nucleon were extracted using QCD analyses. The quark contribution to the proton helicity is now confirmed to be around 0.3, smaller than the expected value of 0.6 [10]. However, due to the limited range in $Q^2$ covered by the experiments at fixed $x_{\mathrm{Bj}}$ the QCD analyses (e.g.[4]) show limited sensitivity to the gluon helicity distribution, $\Delta g(x)$, and its first moment, $\Delta G$. The determination of $\Delta g(x)$ has therefore to be complemented by direct measurements in dedicated experiments.

The gluon polarisation $\langle \Delta g/g \rangle_x$ has been determined from the photon–gluon fusion (PGF) process by HERMES [11], SMC [12] and COMPASS [13]. These analyses used events containing hadron pairs with high transverse momenta, $p_{\mathrm{T}}$, with respect to the virtual photon direction. This method provides good statistical precision but relies on Monte Carlo generators simulating QCD processes. The measurements point towards a small value of the gluon polarisation at $x \approx 0.1$. This is in line with recent results from PHENIX [8] and STAR [9] at RHIC.

In the Quark Parton Model the nucleon spin is given by the quark spins, $\Delta\Sigma$, while $\Delta G$ vanishes. Taking into account orbital angular momenta, $L$, of quarks and gluons the nucleon spin is

$$\frac{1}{2} = \frac{1}{2}\Delta\Sigma + \Delta G + L_z \,. \tag{1}$$

In QCD the U(1) anomaly generates a gluonic contribution to the measured singlet axial coupling, $a_0(Q^2)$. This anomalous gluonic contribution does not vanish at $Q^2 \to \infty$. As a result, $\Delta\Sigma(Q^2)$ becomes scheme dependent and may differ from the observable $a_0$ while $\Delta G$ is scheme–independent at least up to the NLO. In the Adler–Bardeen factorization scheme [14] $\Delta\Sigma^{\mathrm{AB}}$ is independent of $Q^2$. Restoring the Ellis-Jaffe value of $\Delta\Sigma^{\mathrm{AB}} \approx 0.6$ requires a value of $\Delta G(Q^2) \approx 2$ and $L_z \approx -2$ at $Q^2 = 5$ (GeV/$c$)$^2$.

Here, we present a new result on $\langle \Delta g/g \rangle_x$ from muon-deuteron scattering. The gluon polarisation is determined assuming that open charm production is dominated by the PGF mechanism yielding a $c\bar{c}$ pair which fragments mainly into $D$ mesons. This method has the advantage that in lowest order there are no other contributions to the cross section; however, it is statistically limited. In our analysis only one charmed meson is required in every event. This meson is selected through its decay in one of the two channels: $D^*(2010)^+ \to D^0\pi^+_{\mathrm{slow}} \to K^-\pi^+\pi^+_{\mathrm{slow}}$ ($D^*$ sample) and $D^0 \to K^-\pi^+$ ($D^0$ sample) and their charge conjugates.

The data were collected during 2002 to 2004 with the 160 GeV/$c$ CERN SPS $\mu^+$ beam and correspond to an integrated luminosity of 1.7 fb$^{-1}$. The beam muons coming from the $\pi^+$ and $K^+$ decays are naturally polarised with an average polarisation, $P_{\mathrm{b}}$, of about $-80\%$.

The polarised $^6$LiD target consists of two cells (upstream $u$, downstream $d$), each

research funds for 2005-2007
n) Supported by KBN grant nr 134/E-365/SPUB-M/CERN/P-03/DZ299/2000

60 cm long, longitudinally polarised with opposite orientations. The spin directions are reversed every eight hours by rotating the field of the target magnet system. The average target polarisations, $P_{\rm t}$, were $\pm 50\%$. The $^6$Li nucleus basically consists of an $^4$He core plus a deuteron. A dilution factor, $f$, of about 0.4 is obtained for the target material. The exact value is kinematics dependent and is calculated as described in [15]. Particle tracking and identification are performed in a two-stage spectrometer [16].

The present analysis selects events with an incoming muon, a scattered muon identified behind hadron absorbers, an interaction vertex in the target and at least two additional charged tracks. The $D^0$ mesons are reconstructed through their $K\pi$ decay which has a branching ratio of 3.8%. Due to multiple Coulomb scattering of the charged particles in the solid state target the spatial resolution of the vertex reconstruction is not sufficient to separate the $D^0$ production and decay vertices. Therefore, the mesons are reconstructed on a combinatorial basis, considering all pairs of oppositely charged tracks in a given event and calculating their invariant mass. This method results in a high combinatorial background which is reduced in further analysis steps.

The largest background reduction stems from kaon identification in the Ring Imaging CHerenkov counter (RICH). This restricts the studied events to a sample with kaons of momenta exceeding 9.1 GeV/$c$. Simulations have shown that in the acceptance about 70% of kaons coming from $D^0$ decays exceed this threshold.

Particle identification in the RICH starts from reconstructed tracks with measured momenta. The angles between the track and the detected Cherenkov photons are calculated for each track. The comparison of the expected angular distribution of photons for a pion, a kaon or a proton with the measured one is used for particle identification. For this comparison two different methods were used. The data from 2002 and 2003 were analysed using a $\chi^2$ calculated from the photon angles and the Cherenkov angles. The mass hypothesis with the smallest $\chi^2$ is selected. For the 2004 data, the likelihoods for the various mass hypotheses are also compared to the background likelihood. The background likelihood function is evaluated using photons not associated to reconstructed tracks.

In the analysis an identified kaon and an identified pion are required for each event except for the $D^*$ sample analysed with the $\chi^2$ method where all tracks not identified as kaons are considered as pion candidates. The $D^*$ and the $D^0$ samples are analysed independently. The following two kinematic cuts are used for the $D^*$ ($D^0$) sample: a cut $z > 0.2$ ($z > 0.25$), where $z$ is the fraction of the energy of the virtual photon carried by the $D^0$ meson candidate, and a cut $|\cos\theta^*| < 0.85$ ($|\cos\theta^*| < 0.5$), where $\theta^*$ is the decay angle in the $D^0$ c.m.s. system. In the $D^*$ channel a cut on the mass difference is imposed, $3.1\ \mathrm{MeV}/c^2 < M_{K\pi\pi_{slow}} - M_{K\pi} - M_\pi < 9.1\ \mathrm{MeV}/c^2$, where $M_{K\pi\pi_{slow}}$ and $M_{K\pi}$ are the masses of the $D^*$ and the $D^0$ candidates, respectively. The resulting signal-to-background ratio for events in the signal region is approximately 1:1 for the $D^*$ and 1:10 for the $D^0$ sample (Fig. 1). Note that the events entering the $D^*$ sample are not used in the $D^0$ sample.

The number of events, $N$, collected in a given target cell and time interval (about one week of data taking) is

$$N = a\phi n(\sigma_{\rm S} + \sigma_{\rm B}) \times \left[1 + P_{\rm t}P_{\rm b}f\left(a_{\rm LL}\frac{\sigma_{\rm S}}{\sigma_{\rm S}+\sigma_{\rm B}}\left\langle\frac{\Delta g}{g}\right\rangle_x + D\frac{\sigma_{\rm B}}{\sigma_{\rm S}+\sigma_{\rm B}}A_{\rm B}\right)\right] . \quad (2)$$

Here, $a$, $\phi$ and $n$ are the spectrometer acceptance, the integrated incident muon flux and the number of target nucleons, respectively. In addition $\sigma_{\rm S}$ ($\sigma_{\rm B}$) is the cross section of the

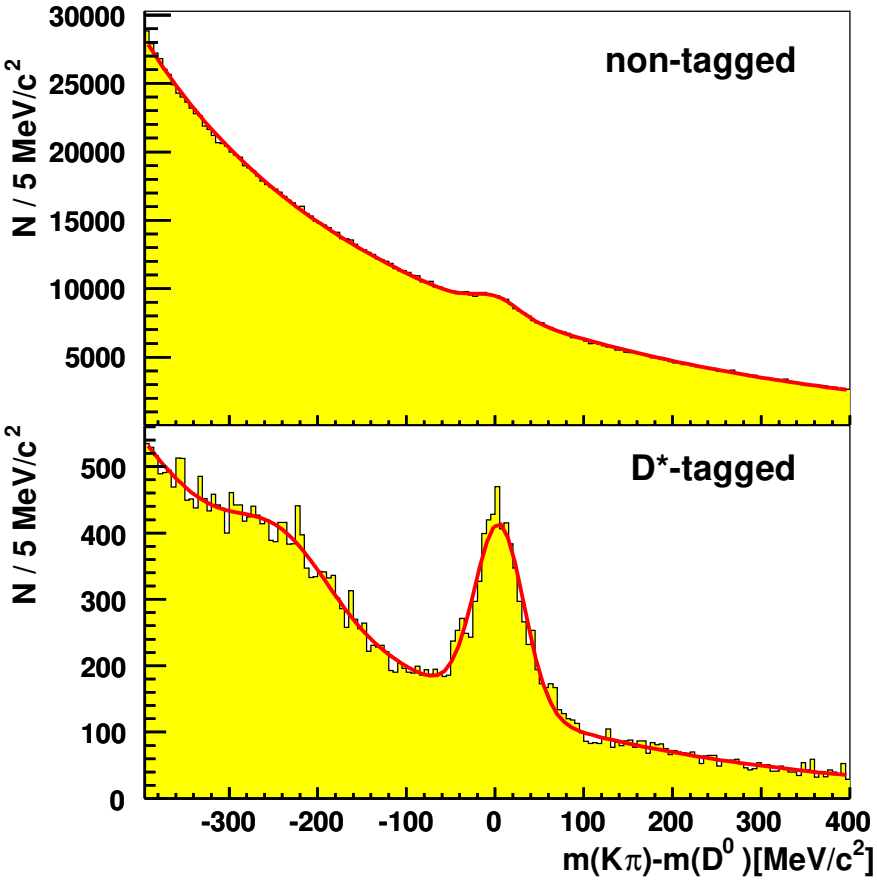


Figure 1: Invariant mass distributions of the $K\pi$ pairs tagged with the $D^*$ decay ($D^*$ sample, lower) and of the non-tagged $K\pi$ pairs ($D^0$ sample, upper). The curves represent fits with functional form described in the text.

events described by the central Gaussians (background) in Fig. 1. The analysing power $a_{\rm LL}$ is the asymmetry for the $\mu g \to \mu c\bar{c}$ process, and $A_{\rm B}$ the background asymmetry. The depolarisation factor, $D$, from Ref. [17] is used.

A simultaneous extraction of $\langle \Delta g/g \rangle_x$ and $A_{\rm B}$, assumed to be constant in the mass range considered, is performed independently for the $D^*$ and the $D^0$ sample using the events in the mass range $-400$ MeV/$c^2$ $< M_{D^0} - M_{K\pi} <$ 400 MeV/$c^2$ recorded in the two target cells before ($u$,$d$) and after ($u'$,$d'$) target spin reversal. The events of the four samples are weighted with a signal weight, $w_{\rm S}$, and independently with a background weight, $w_{\rm B}$,

$$w_{\rm S} = P_{\rm b} f a_{\rm LL} \frac{\sigma_{\rm S}}{\sigma_{\rm S} + \sigma_{\rm B}} \ , \ w_{\rm B} = P_{\rm b} f D \frac{\sigma_{\rm B}}{\sigma_{\rm S} + \sigma_{\rm B}} \ . \tag{3}$$

The target polarisation is not included into the weights because it is time dependent. In this way 8 equations

$$\sum_{i=1}^{N_t} w^t_{{\rm C},i} = \alpha^t_{\rm C} \left( 1 + \beta^t_{\rm C} \left\langle \frac{\Delta g}{g} \right\rangle_x + \gamma^t_{\rm C} A_{\rm B} \right) \tag{4}$$

with

$$\beta^t_{\rm C} = \frac{\sum_i^{N_t} P_{{\rm t},i} w^t_{{\rm S},i} w^t_{{\rm C},i}}{\sum_i^{N_t} w^t_{{\rm C},i}} \ , \ \gamma^t_{\rm C} = \frac{\sum_i^{N_t} P_{{\rm t},i} w^t_{{\rm B},i} w^t_{{\rm C},i}}{\sum_i^{N_t} w^t_{{\rm C},i}} \tag{5}$$

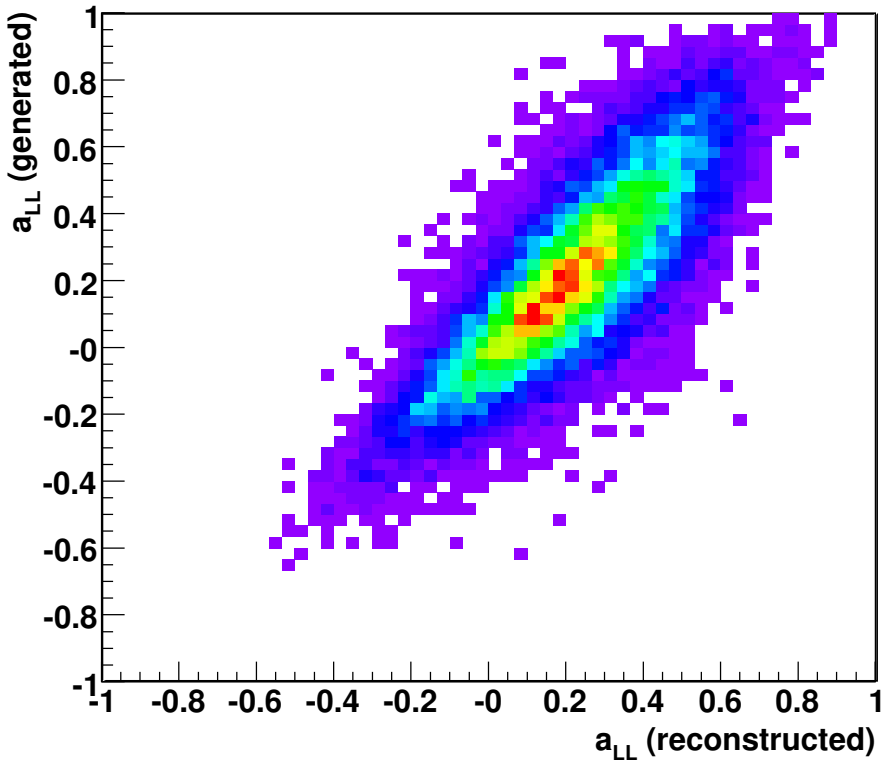


Figure 2: Correlation between generated and reconstructed values of $a_{\mathrm{LL}}$.

are obtained from Eq. (2) for the 10 unknowns which are $\langle \Delta g/g \rangle_x$ , $A_{\mathrm{B}}$ and 8 acceptance factors $\alpha^t_{\mathrm{C}} = \int a^t \phi^t n^t (\sigma_{\mathrm{S}} + \sigma_{\mathrm{B}}) w^t_{\mathrm{C}} \mathrm{d}X$ with $t = u, d, u', d'$ and $\mathrm{C} = \mathrm{S}, \mathrm{B}$ [18]. Here, $\int \mathrm{d}X$ stands for the integration over the accessible kinematic region. Assuming that possible acceptance variations affect the upstream and downstream cells in the same way, i.e. $\alpha^u_{\mathrm{C}}/\alpha^d_{\mathrm{C}} = \alpha^{u'}_{\mathrm{C}}/\alpha^{d'}_{\mathrm{C}}$, provides two additional equations (as in Refs. [4, 17]). With an extra, much weaker, assumption that signal and background events on the same target cell are affected in the same way by the acceptance variations one finally arrives at a system of 8 equations with 7 unknowns. Possible deviations from the above assumptions generate false asymmetries which are included in the systematic error.

For the evaluation of Eq. (4) $P_{\mathrm{b}}$ is parameterized as a function of the beam momentum. For $P_{\mathrm{t}}$, values averaged over about one hour are used. The signal purity $\sigma_{\mathrm{S}}/(\sigma_{\mathrm{S}} + \sigma_{\mathrm{B}})$, is obtained from a fit to the $M_{K\pi} - M_{D^0}$ spectra. The fit is done separately for the events originating from the two target cells as well as for five (three) separate bins of $f P_{\mathrm{b}} a_{\mathrm{LL}}$ for the $D^*$ ($D^0$) sample. This takes care of the correlation between the signal purity and the analysing power. The spectra are fitted by the sum of signal and background functions, described by a Gaussian and a product of an exponential and a polynomial, respectively. In case of the $D^*$ sample a second Gaussian is used to describe the reflection of $D^0 \rightarrow K\pi\pi^0$ decay, where the $\pi^0$ meson is not observed. In the $D^0$ sample this reflection is not visible. The total number of $D^0$ mesons is about 3,800 and 13,800 in the $D^*$ and the $D^0$ samples, respectively.

Finally, the determination of $\langle \Delta g/g \rangle_x$ requires knowledge of the analysing power $a_{\mathrm{LL}}$. Since only one $D^0$ is measured, the partonic kinematics cannot be fully reconstructed and $a_{\mathrm{LL}}$ cannot be calculated on an event-by-event basis. A kinematic factor which is approximately equal to the depolarisation factor $D$ is factored out and the remaining

Table 1: Systematic error contributions to $\langle \Delta g/g \rangle_x$ .

| source | $\delta(\frac{\Delta g}{g})$ | source | $\delta(\frac{\Delta g}{g})$ |
|---|---|---|---|
| False asymmetry | 0.09 | Beam polarization $P_{\mathrm{b}}$ | 0.02 |
| Fitting | 0.09 | Target polarization $P_{\mathrm{t}}$ | 0.02 |
| Binning | 0.04 | Dilution factor $f$ | 0.02 |
| MC parameters | 0.05 | | |
| | Total error | 0.15 | |

part of $a_{\mathrm{LL}}$ is parameterized in terms of measured kinematic variables. This is done using a neural network trained on a Monte Carlo (MC) sample for $D^*$ mesons. The correlation between the generated and the reconstructed $a_{\mathrm{LL}}$ is 82% (see Fig. 2). The sample was generated with AROMA [19] in leading order QCD and the events were processed by GEANT to simulate the response of the detector and finally reconstructed like real events. The scale, $\mu^2$, used in the MC simulation was determined by the mass of the produced charm quark pair and is sufficiently large to justify the perturbative approach.

The gluon polarisation $\langle \Delta g/g \rangle_x$ is determined for each of the 29 weeks of data taking with a standard least square minimisation procedure taking into account the statistical correlation between events weighted by $w_{\mathrm{S}}$ and by $w_{\mathrm{B}}$. As in our inclusive analysis [4] the event weighting reduces the statistical error. The final value for $\langle \Delta g/g \rangle_x$ is the weighted mean of the above results. The resulting $A_{\mathrm{B}}$ is consistent with zero. Note that we measure $\Delta g/g$ in a given range of $x$. Provided that $\Delta g/g(x)$ is weakly dependent on $x$ in the range covered, this method gives a measurement of $\Delta g/g(\langle x \rangle)$, where $\langle x \rangle$ is calculated with signal weights. The above assumption is supported by the results of our QCD analysis [4].

The major contributions to the systematic error are listed in Table 1. The contributions from $P_{\mathrm{b}}$, $P_{\mathrm{t}}$ and $f$ are as discussed in [4]. To study the influence of false asymmetries the final samples from Fig. 1 were subdivided into two samples using criteria related to the experimental apparatus, e.g. kaons going to the upper or to the lower spectrometer parts. The resulting asymmetries were found to be compatible within their statistical accuracy, thus no false asymmetries were observed. The upper limit of the contribution to the systematic error was also estimated from the dispersion of the values for $\langle \Delta g/g \rangle_x$ and $A_B$ for the various data taking week. Assuming that possible detector instabilities are similar for background and signal events and applying a method as in [4] leads to a conservative limit of 0.09 for both decay channels. The fit for the signal purity determination was performed with different background parameterizations, different binnings for the invariant mass spectra and varying the constraints for some of the fit parameters. The resulting dispersion of the $\langle \Delta g/g \rangle_x$ values was 0.09 for both channels. The $\langle \Delta g/g \rangle_x$ calculations were repeated with several sets of binning in $f P_b a_{\mathrm{LL}}$ and the dispersion of the results was 0.04 for both channels. Other contributions like radiative corrections and event migration between target cells are negligible. All these studies were done independently for the $D^0$ and $D^*$ samples and result in very similar values for all the contributions. To estimate the influence of the simulation parameters, i.e. charm quark mass (1.3 GeV/$c^2$ to 1.6 GeV/$c^2$) and parton distribution functions, MC samples with different parameter sets were generated and $a_{\mathrm{LL}}$ was recalculated. The dispersion of the resulting $\langle \Delta g/g \rangle_x$ for the combined $D^0$ and $D^*$ sample was 0.05. In addition, it was checked that the parameterization of $a_{\mathrm{LL}}$ is valid for the $D^0$ and the $D^*$ sample. The resolved photon contribution to the open charm

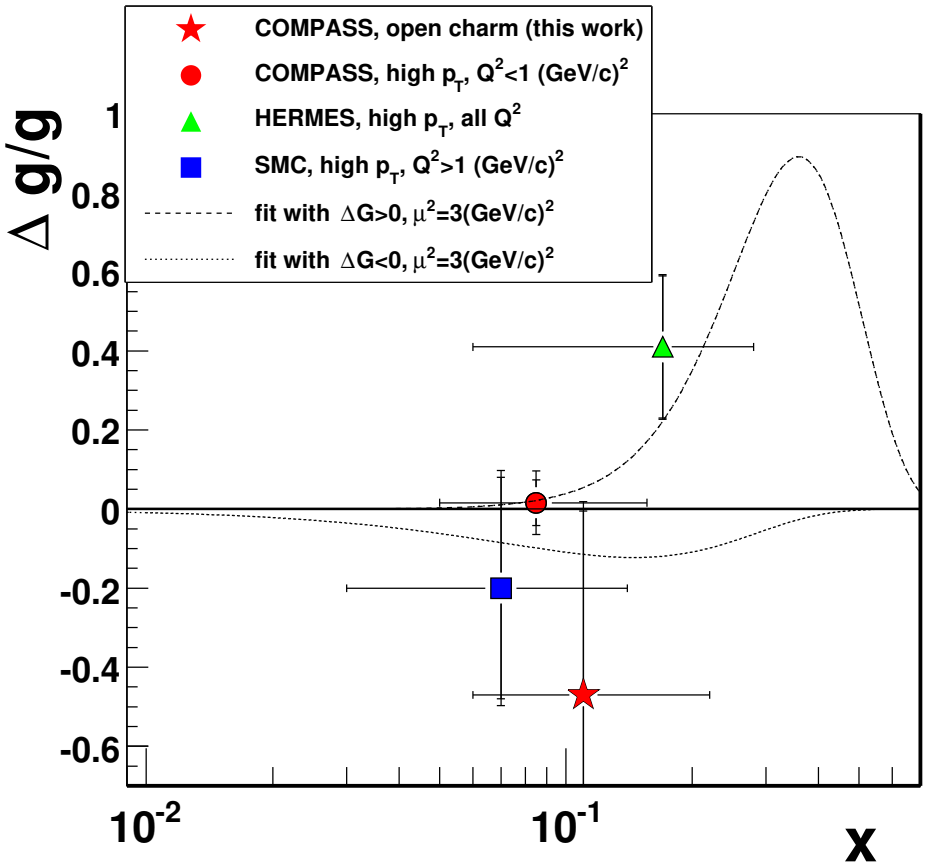


Figure 3: Compilation of the $\langle \Delta g/g \rangle_x$ measurements from open charm and high $p_{\mathrm{T}}$ hadron pair production by COMPASS [13], SMC [12] and HERMES [11] as a function of $x$. Horizontal bars mark the range in $x$ for each measurement, vertical ones give the statistical precision and the total errors (if available). The open charm measurement is at a scale of about 13 $(\mathrm{GeV}/c)^2$, other measurements at 3 $(\mathrm{GeV}/c)^2$. The curves display parameterizations from a NLO QCD analysis in the $\overline{\mathrm{MS}}$ scheme at 3 $(\mathrm{GeV}/c)^2$, [4]: fits with $\Delta G > 0$ (broken line) and with $\Delta G < 0$ (dotted line).

production via gluon-gluon fusion has been estimated with the RAPGAP generator [20] and found to be negligible in our kinematic range.

The values obtained for $\langle \Delta g/g \rangle_x$ are $0.53 \pm 0.75(\mathrm{stat})$ for the $D^0$ and $-1.01 \pm 0.55(\mathrm{stat})$ for the $D^*$ sample. These two values agree within 1.7 standard deviations and their weighted mean is

$$\left\langle \frac{\Delta g}{g} \right\rangle_x = -0.47 \pm 0.44(\mathrm{stat}) \pm 0.15(\mathrm{syst})$$

at a value of $\langle x \rangle = 0.11^{+0.11}_{-0.05}$ and a scale $\langle \mu^2 \rangle \approx 13$ $(\mathrm{GeV}/c)^2$. All the contributions to the systematic error in Table 1 were added in quadrature and conservatively assumed to be fully correlated in the two samples.

In Fig. 3 the above result is compared to other measurements of $\langle \Delta g/g \rangle_x$ and to parameterizations from a QCD analysis of the structure function data [4]. It is in good agreement with previous measurements favouring small values of $\langle \Delta g/g \rangle_x$ . Note that the scale here is $\mu^2 \approx 13$ $(\mathrm{GeV}/c)^2$ while all other points and the curves are given at $\mu^2 \approx 3$ $(\mathrm{GeV}/c)^2$.

In summary, we have performed the first determination of $\langle \Delta g/g \rangle_x$ from a measurement of the cross section asymmetry for $D^0$ meson production. In the analysis photon–gluon fusion in LO QCD was assumed to be the underlying production mechanism for open charm production. The resulting value of $\langle \Delta g/g \rangle_x$ is compatible with our previous result from high $p_{\mathrm{T}}$ hadron pairs but is less model dependent.

We acknowledge the support of the CERN management and staff, the special effort of CEA/Saclay for the target magnet project, as well as the skills and efforts of the technicians of the collaborating institutes.

**References**

[1] V.W. Hughes, Nucl. Phys. A **518** (1990) 371 and references therein.
[2] EMC, J. Ashman *et al.*, Nucl. Phys. B **328** (1989) 1; Phys. Lett. B **206** (1988) 364.
[3] SMC, B. Adeva *et al.*, Phys. Rev. D **58** (1998) 112001.
[4] COMPASS, V.Yu. Alexakhin *et al.*, Phys. Lett. B **647** (2007) 8.
[5] E155, P. L. Anthony *et al.*, Phys. Lett. B **463** (1999) 339; see also list of references in [4].
[6] HERMES, A. Airapetian *et al.*, Phys. Rev. D **75** (2007) 012007; erratum *ibid.* D**76** (2007) 039901.
[7] JLAB/Hall A Collaboration, X. Zheng *et al.*, Phys. Rev. Lett. **92** (2994) 012004.
[8] PHENIX, S. S. Adler *et al.*, Phys. Rev. D **73** (2006) 091102(R); A. Adare *et al.*, arXiV:0704.3599.
[9] STAR, B. I. Abelev *et al.*, Phys. Rev. Lett. **97** (2006) 252001.
[10] J. Ellis, R. Jaffe, Phys. Rev. **D** (1974) 1444; **10** (1974) 1669.
[11] HERMES, A. Airapetian *et al.*, Phys. Rev. Lett. **84** (2000) 2584; recently a smaller preliminary value from another method has been reported in P. Liebig, AIP Conf. Proc. **915** (2007) 331 (arXiv:0707.3617).
[12] SMC, B. Adeva *et al.*, Phys. Rev. D **70** (2004) 012002.
[13] COMPASS, E.S. Ageev *et al.* Phys. Lett. B **633** (2006) 25.
[14] R.D. Ball, S. Forte and G. Ridolfi, Phys. Lett. B **378** (1996) 255.
[15] COMPASS, E.S. Ageev *et al.*, Phys. Lett. B **612** (2005) 154.
[16] COMPASS, P. Abbon *et al.* Nucl. Instr. Meth. A **577** (2007) 455.
[17] COMPASS, V.Yu. Alexakhin *et al.*, Phys. Lett. B **647** (2007) 330.
[18] For details see: J. Pretz, habilitation thesis, University of Bonn (2007).
[19] G. Ingelman, J. Rathsman and G. A. Schuler, Comput. Phys. Commun. **101** (1997) 135; see http://www.isv.uu.se/thep/aroma/ for recent updates.
[20] H. Jung, Comput. Phys. Commun. **86** (1995) 147; see www.desy.de/∼jung/rapgap for recent updates.